

Article

Foam Glass Crystalline Granular Material from a Polymineral Raw Mix

Olga Miryuk ¹, Roman Fediuk ^{2,*} and Mugahed Amran ^{3,4}¹ Rudny Industrial Institute, Rudny 111500, Kazakhstan; psm58@mail.ru² Polytechnic Institute, Far Eastern Federal University, 690922 Vladivostok, Russia³ Department of Civil Engineering, College of Engineering, Prince Sattam Bin Abdulaziz University, Alkharj 11942, Saudi Arabia; m.amran@psau.edu.sa⁴ Department of Civil Engineering, Faculty of Engineering and IT, Amran University, Amran 9677, Yemen

* Correspondence: fedyuk.rs@dvvfu.ru

Abstract: The article is devoted to the development of resource-saving technology of porous granular materials for energy-efficient construction. The relevance of the work for international research is to emphasize expanding the raw material base of porous lightweight concrete aggregates at the expense of technogenic and substandard materials. The work aims to study the processes of porization of glass crystalline granules from polymineral raw materials mixtures. The novelty of the work lies in the establishment of regularities of thermal foaming of glass crystalline granules when using waste of magnetic separation of skarn-magnetite (WMS) ores and lignite clay. Studies of liquid glass mixtures with various mineral fillers revealed the possibility of the formation of a porous structure with the participation of opoka, WMS and lignite clay. This is due to the presence in the materials of substances that exhibit thermal activity with the release of a gas phase. The foaming efficiency of the investigated materials increases when combined with glass breakage. The addition of WMS and lignite clay to the glass mixture increases the pore size in comparison with foam glass. The influence of the composition of raw mixtures on the molding and stability of granules is determined. The addition of sodium carbonate helps to strengthen the raw granules and reduce the softening temperature of the mass. The composition of the molding mixture of glass breakage, liquid glass and a multicomponent additive is developed, which provides an improvement in the molding properties of the glass mass, foaming of granules at a temperature of 750 °C. Foam glass crystalline granules have polymodal porosity, characterized by a density of 330–350 kg/m³, a compressive strength of 3.2–3.7 MPa, and a thermal conductivity of 0.057–0.061 W/(m·°C). Accordingly, the developed granules have a high potential use in structural and heat-insulating concretes.

Keywords: crystalline granular material; man-made materials; blowing agents; thermal foaming; porous structure



Citation: Miryuk, O.; Fediuk, R.; Amran, M. Foam Glass Crystalline Granular Material from a Polymineral Raw Mix. *Crystals* **2021**, *11*, 1447. <https://doi.org/10.3390/cryst11121447>

Academic Editor:
Yurii Barabanshchikov

Received: 24 October 2021
Accepted: 22 November 2021
Published: 24 November 2021

Publisher's Note: MDPI stays neutral with regard to jurisdictional claims in published maps and institutional affiliations.



Copyright: © 2021 by the authors. Licensee MDPI, Basel, Switzerland. This article is an open access article distributed under the terms and conditions of the Creative Commons Attribution (CC BY) license (<https://creativecommons.org/licenses/by/4.0/>).

1. Introduction

An important stage of technology that provides building materials with a decrease in density, thermal insulation and acoustic properties, is the formation of a porous structure. Foaming is a common method of forming pores and is implemented in the technology of cellular concrete [1–3], porous granular and composite materials [4]. Foaming occurs by saturation of the viscous-plastic raw material mass with the gas phase, which forms spherical pores [5]. The nature of porosity depends on the composition and condition of the raw material [6]. The leading positions of heat-insulating materials made of silicate glasses are due to a highly porous structure that is resistant to physical and mechanical influences [7]. Porous materials from silicate glasses are produced in the form of piece products (blocks, slabs and others) [8] and granules used as a filler for lightweight concrete and heat-insulating backfills [9].

A representative of porous silicate glasses is cellular glass or foam glass, characterized by the presence of up to 80–90% of spherical or hexagonal pores, 0.5–1.5 mm in size [10]. Foam glass is obtained by thermal foaming of a special glass mass containing a blowing agent [11]. The shortage of raw materials and the multistage processing of molten glass [12–14] hinder the widespread use of traditional technology of foam glass. The use of secondary glass breakage is aimed at reducing the shortage of raw materials, reducing the energy intensity of production. However, it is accompanied by other technological problems. The instability of the composition of glass breakage of various origins, the lack of a clearly organized mass collection of glass breakage in most regions of the country cause a decrease in the quality of foam glass [15]. The formation of pores in the foam glass occurs due to the introduction of blowing agents. The type and amount of the blowing agent significantly affects the nature of the porosity of the foam glass. For example, the use of carbonate blowing agents provides a large-pore structure and the presence of interconnected pores. The structure of the foam glass with the use of solid carbonaceous blowing agents is characterized by fine uniform porosity. The content of solid blowing agents in the raw mixture is on average 5–10% [16]. Uniform distribution of the gas-forming additive is achieved with fine joint grinding with the glass component of the raw mixture, which often leads to a loss of activity of the pore-forming component. To regulate the rheological properties of the glass mass, alkaline earth components, for example, dolomite and limestone rocks, are introduced into the raw mixture. To reduce the temperature of formation of the pyroplastic state, compounds of boron, sodium, and potassium are added to the raw material mass. Consequently, to obtain foam glass, a raw mixture of a complex chemical composition is required.

At present, along with traditional foam glass, technologies of foam glass crystalline materials and foam glass ceramics are being developed [17–19]. The presence of a crystalline phase in a porous glassy matrix is achieved by changing the composition of the raw mixture and improves the quality of porous silicate glasses. To obtain foam-glass-crystalline materials, silica-containing rocks and man-made materials are widely used [20]. Another type of porous silicate glasses are materials based on liquid glass [21]. Liquid glass is an aqueous solution of alkaline silicates characterized by chemical activity, controlled density, astringent properties, and high sensitivity to thermal effects [22]. When heated to 120–500 °C, liquid glass is capable of forming solid foam with a density of 50–150 kg/m³. The combination of liquid glass with fillers makes it possible to create materials with a highly porous cellular structure. Physicochemical characteristics of liquid glass provide numerous options for foaming in the technologies of aerated concrete, granules of various sizes and purposes [23]. The technology of porous liquid glass compositions is characterized by low energy consumption. Expanded liquid glass materials are favorably distinguished by increased porosity and reduced density. However, they are inferior to other porous glasses in terms of strength and water resistance. The unique properties of liquid glass are also realized in foam glass technology. Liquid glass is a multifunctional component of the raw mixture: at the stage of molding it facilitates binding of the powder mass; during heat treatment, it reduces the softening temperature of the molten glass and ensures the formation of porosity. During the chemical interaction of liquid glass and glass powder, silicates are formed containing bound water, which serves as a source of the gas phase for foaming the glass mass [22].

In recent years, the development of foam glass materials has been quite intensive. The team of König and Petersen is the leading team in foam glass developments [10,12,13,24]. They investigated the use of foam-oxidant pairs for the formation of foam glass [24]. In addition, this team carried out modeling of heat transfer mechanisms in recycled foam glass [10]; studied in detail glass foam with macroporosity using glass waste and sodium hydroxide as a foaming agent [11]; investigated the effect of the size of glass particles on the foaming process and physical characteristics of foam glass [12]; and also proved the applicability of liquid glass to transfer the glass foaming process from a controlled atmosphere to an air one [13]. Hesky et al. worked on the development of liquid glass

mixtures for the production of foam glass [25]. Goltsman et al. studied the role of liquid glass in the synthesis of foam glass using a glycerol-based blowing agent [26]. Bernardo et al. studied in detail Biosilicate glass-ceramic foams obtained as a result of the activation of refined alkalis and gel casting [27]. Siddika et al. reviewed the parameters, productivity and problems of powder sintering and gel casting in the manufacture of foam glass using liquid glass [28]. Vaysman et al. studied the recycling of foam glass in the production of building materials [29]. Akai et al. studied in detail the formation of light-colored foam glass from colored cullet [30]. Liu et al. studied the factors influencing the properties of foam glass from glass breakage [31]. Kim et al. have been developing and studying the properties of foam glass with the addition of polysiloxane [32]. Kazmina et al. studied the issues of strengthening foam glass materials [33]. Her team developed a number of compositions for low-temperature foam glass synthesis based on a number of natural and industrial raw materials.

The development of energy-efficient construction technologies is driving the interest in lightweight concrete [34,35]. Adhikary et al. investigated the effect of carbon nanotubes on lightweight concrete based on foam glass and silica aerogel [36]. Granular porous silicate materials are characterized by a rigid cellular structure. Expanded clay gravel, granulated foam glass, and porous granules of expanded liquid glass are used as aggregates for lightweight concrete [37,38]. However, expanded clay does not provide low-density concrete [37]. The structure of expanded liquid glass granules is unstable in composite materials [39].

Numerous developments in recent years are devoted to expanding the raw material base of porous aggregates for lightweight concrete [40–45]. The technology of granulated glass-ceramic foam materials from silica industrial waste is actively developing [46,47]. To obtain aggregates, ash from coal combustion is used [48,49], associated materials from the extraction and processing of ores and fuel, and metallurgical slags [50–56]. A number of developments are devoted to highly porous granular materials based on thermal foaming of liquid glass [57]. The use of new types of raw materials made it possible to improve the technology and create effective porous granular materials with a density of 300–500 kg/m³ [58].

However, the list of studied raw materials remains limited, which prevents the widespread use of the technology of glass-ceramic foam materials [59–62]. The depletion of natural raw material reserves increases the urgency for the active development of man-made sources. For the effective use of new raw materials, it is necessary to develop ideas about the laws of formation of a porous structure, the properties of materials.

The aim of the work is to study the effect of the material composition of the raw mixture on the formation and properties of glass-ceramic foam granules using technogenic materials of various origins. However, to achieve this aim, the following tasks have been identified:

- Study of the effect of mineral additives on thermal transformations of glass mass;
- Research of the processes of formation of a porous structure during the firing of mixtures of various compositions;
- Study of the structure and properties of expanded granular materials.

The research based on a hypothesis providing for the preparation of a glass crystalline mix from components containing gas-forming substances. The combination of raw materials with different thermal stabilities will ensure the gradual saturation of the viscous-plastic mass with the gas phase and the formation of a highly porous structure of the material. The object of the study was glass-crystalline raw mixtures fired at different temperatures. The subject of research is the processes of formation of a highly porous structure, physical and mechanical properties of porous glass-crystalline granular material.

2. Materials and Methods

2.1. Characteristics of the Raw Materials Used

As components of raw mixtures, the following materials were used, the thermal dissociation of which is accompanied by the formation of a gas phase: glass breakage, opoka, waste of magnetic separation of skarn-magnetite ores (WMS), lignite clay, and liquid glass. Figure 1 presents the appearance of all raw materials used. The chemical composition of solid materials is shown in Table 1.



Figure 1. Appearance of the raw materials used: (a) glass breakage, (b) opoka, (c) WMS, (d) lignite clay, (e) liquid glass.

Table 1. Chemical composition of the used raw materials, %.

Material	SiO ₂	Al ₂ O ₃	Fe ₂ O ₃	CaO	MgO	SO ₃	K ₂ O + Na ₂ O	Other	LOI
Breakage sheet glass	69.7–71.8	2.0–5.3	0.1–0.9	4.1–6.7	3.1–4.1	0.3–0.5	13.3–14.8	0.4	0
Breakage glass containers	69.4–71.5	3.3–5.5	0.6–1.2	5.2–5.6	3.2–4.3	0.2–0.4	14.1–16.0	0.2	0
Opoka	80.7	5.2	2.8	0.8	0.7	1.4	1.1	0.5	6.8
WMS	40.3–41.7	12.3–12.9	15.8–16.5	12.1–12.5	6.4–6.5	6.7–6.8	2.5–2.6	1.3–1.5	2.5–2.6
Lignite clay	12.7	47.7	3.5	0.6	0.3	6.7	0.8	0.4	27.3

Glass breakage (sodium-calcium-silicate) is made up of fragments of sheet glass and glass containers at a ratio of 1:1. The basis of technogenic glass is formed by amorphous silica. When heated to a temperature of 750–800 °C, glass breakage turns into a pyroplastic mass capable of foaming. The cooled glass breakage melt includes a small number of small pores due to the gas phase contained in the material.

The opoka used in the work was taken from the Sokolovsko-Sarbaysky deposit (Kazakhstan). Opoka sedimentary rock is composed mainly of amorphous opal including the cristobalite, tridymite and admixtures of clay minerals. The heating of the opoka rock is accompanied by a smooth dehydration of minerals; the bulk of the water is removed at a temperature of 450–500 °C. The work used opoka rock, extracted as overburden during the extraction of minerals.

Waste from magnetic separation of skarn-magnetite ores is a technogenic material formed during the dressing of iron ore at the largest mining and processing enterprise, Sokolovsko-Sarbaysky, in Kazakhstan. The mineral basis of ore dressing wastes is composed of calcium-magnesium silicates and aluminosilicates, differing in genesis, composition, structure, chemical activity, and thermal stability. The chemical composition listed in Table 1 was determined using X-ray diffraction. Pyroxenes, garnets, amphiboles, feldspars, chlorites, epidote, and scapolite dominate the technogenic material [15,23]. Waste also contains pyrite, calcium carbonate, magnetite, and quartz [26].

The mineral composition of the skarn-magnetite ore dressing wastes was determined by petrographic analysis performed earlier by the authors using equipment from the geological laboratory of the mining and processing enterprise [23]. According to petrographic analysis, the content of minerals in the WMS, %, are: pyroxenes 20–25, garnets 7–12, amphiboles 7–14, feldspars 8–12, chlorites 7–10, epidote 10–13, scapolite 8–11, pyrite 4–8, calcite 4–7, magnetite 3–4, and quartz 2–4. X-ray phase analysis confirmed the results of

petrographic studies. By the diffraction pattern of the WMS (Figure 2), pyroxenes were diagnosed: diopside ($d = 0.318, 0.299, 0.252$ nm) and augite ($d = 0.299, 0.152$ nm); garnets: andradite ($d = 0.268, 0.244, 0.191$ nm) and grossular ($d = 0.298, 0.268, 0.160$ nm); feldspars: albite ($d = 0.400, 0.318, 0.299$ nm) and anorthite ($d = 0.320, 0.250$ nm); amphibole: actinolite ($d = 0.834, 0.312, 0.284$ nm); epidote ($d = 0.350, 0.290$ nm), and scapolite ($d = 0.327, 0.298, 0.257$ nm); chlorites ($d = 1.360, 0.725, 0.353$ nm); pyrite ($d = 0.163$ nm); calcite ($d = 0.303$ nm); quartz ($d = 0.335$ nm); and magnetite ($d = 0.255$ nm). Studies of thermal transformations in WMS have expanded the understanding of polymineral technogenic material (Figure 3).

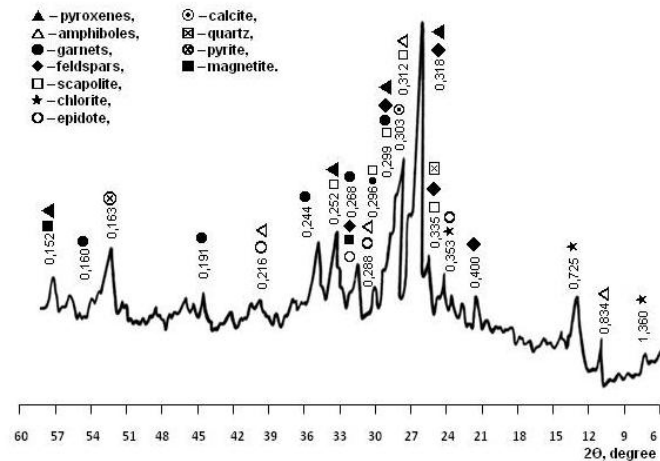


Figure 2. XRD pattern of WMS.

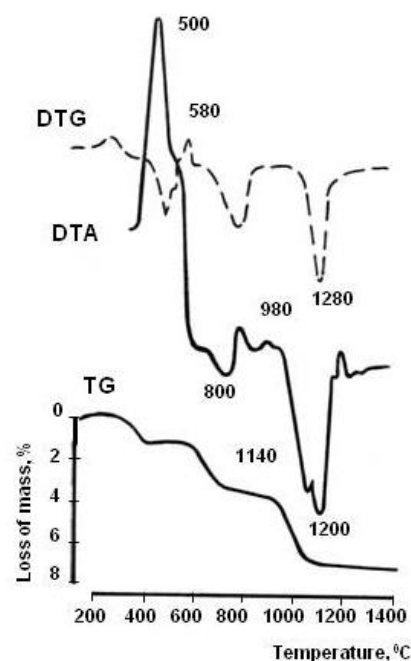


Figure 3. DTG pattern of WMS.

The polymineral composition of the technogenic material determined the stepwise nature of thermal transformations, identified by the method of differential thermal analysis [28]. Pyrite and magnetite are oxidized in the temperature range 400–600 °C, as evidenced by the exothermic effect. When the temperature rises to 600–800 °C, calcite decarbonization occurs, intensified by pyrite decomposition products; dehydration of amphiboles, chlorite, and epidote. Endothermic processes in the temperature range 800–900 °C are caused by the destruction of the crystal structures of amphiboles, chlorite, epidote,

and scapolite. At a temperature of 1000–1200 °C, a silicate melt is formed. Due to the presence of numerous modifying elements in the chemical composition of ore dressing wastes (TiO₂—0.53%, P₂O₅—0.30%, MnO—0.35%, V₂O₅—0.06%, Cl—0.09%, Cu—0.05%, Ni—0.008%) the melt has a low viscosity.

The lignite clay used in the work was taken from the Rudny deposit (Kazakhstan). Lignite clay is a high-alumina rock of sedimentary origin, containing carbonized wood. The mineral base of lignite clay is formed by kaolinite and aluminum hydroxides (hydrargillite and boehmite). According to thermogravimetric data, the bulk of the mass loss of lignite clay due to the removal of the gas phase is noted in the temperature range of 200–550 °C and is associated with the dehydration of aluminum hydroxides and the combustion of plant substances. Lignite clay forms deposits near bauxite deposits in Kazakhstan. The presence of fragments of carbonized wood excludes the use of high-alumina lignite rock in the production of aluminum.

Liquid glass is an aqueous solution of sodium silicate (Na₂O·mSiO₂ + nH₂O). Liquid glass with a silicate modulus 2.8 and density 1350–1400 kg/m³ was introduced as a binder for the powdery raw mixture and a pore-forming agent for the glass crystalline mass. The use of glass breakage, opoka rock, and liquid glass to obtain foam glass materials is known from scientific and technical literature and production experience [58]. Waste from magnetic separation of skarn-magnetite ores and lignite clay as raw materials of glass-crystalline charge were also studied for the first time.

2.2. Mix Design

To achieve the aim of the article, the design of the compositions is detailed in Table 2. The marking of the samples reflects the peculiarities of the composition of the raw mixtures. The raw mixture containing glass breakage as filler is designated C. Raw mixtures C1, C2, and C3 differ from the raw mixture with the content of an additional component (Table 2). Raw mixes of the CB series contain multicomponent filler. The raw mixtures designated CB11, CB21, and CB31 differ from the raw mixtures CB1, CB2, and CB3 by the presence of the addition of Na₂CO₃.

Table 2. Mix proportions.

Mix ID	Raw Mix Composition, %				Na ₂ CO ₃ Content, %	The Amount of Liquid Glass in the Molding Mass, %	Plastic Strength of the Molding Mass, MPa
	Glass Breakage	Opoka	WMS	Lignite Clay			
C	100	0	0	0	0	40	0.070
C1	80	20	0	0	0	40	0.082
C2	80	0	20	0	0	40	0.027
C3	80	0	0	20	0	40	0.042
CB1	60	20	20	0	0	45	0.051
CB11	60	20	20	0	3	45	0.072
CB2	60	20	0	20	0	45	0.065
CB21	60	20	0	20	3	45	0.083
CB3	60	13	15	12	0	45	0.057
CB31	60	13	15	12	3	45	0.075

2.3. Laboratory Equipment and Research Methods

Figure 4 presents the flowchart of the conducted studies.

The glass breakage and opoka were preliminarily crushed by an Udarnik-18 disintegrator (Altaystroy Mash, Barnaul, Russia).

The experimental research methodology provided for the grinding of raw materials to a specific surface area of 450–500 m²/kg. The solid components of the raw mixture were milled together in an Emax laboratory high-speed vibration mill (Retsch, Germany). The productivity of the mill for this type of raw material was 1 L in 10 min. The specific surface of the powders was measured on an FSH-6K photo sedimentometer (Pribory Khodakova, Russia).

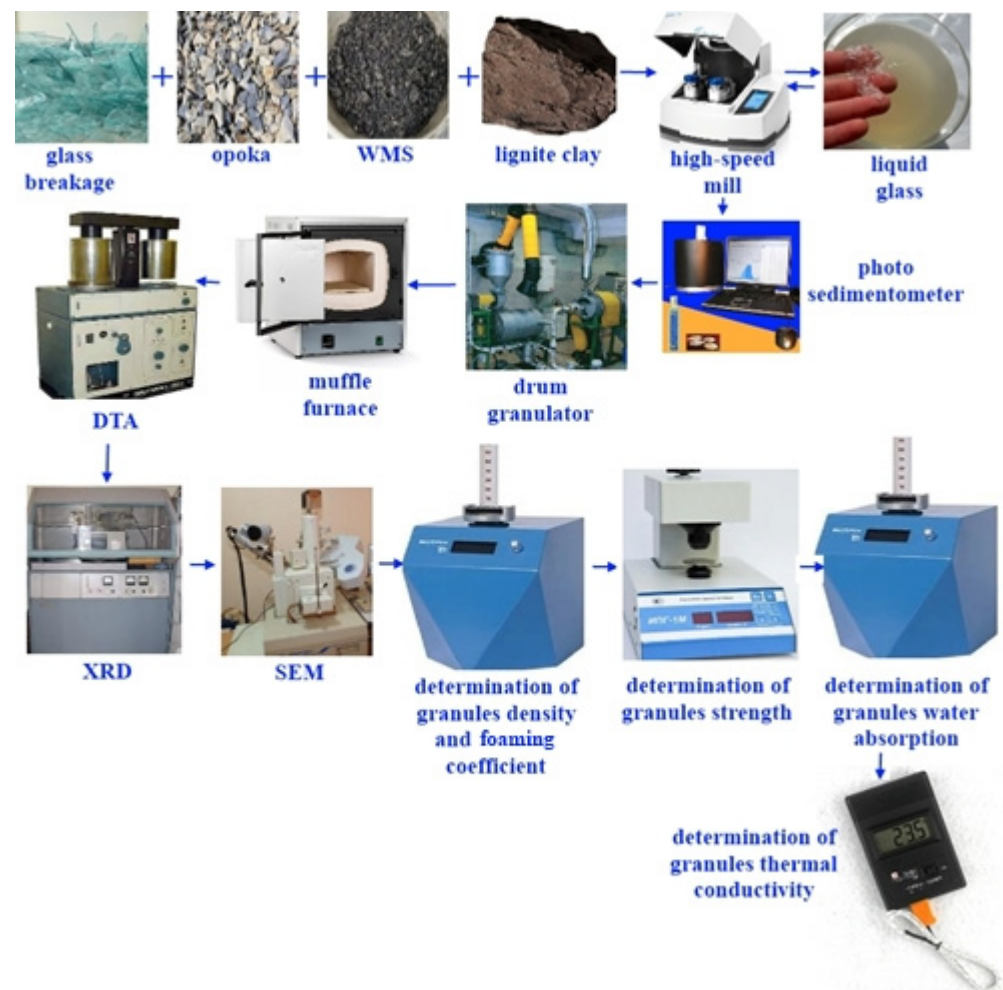


Figure 4. Flowchart of the conducted studies.

Liquid glass was introduced into the prepared raw material mass, and then the mixture was thoroughly mixed. The state of the molding mixture was monitored using a conical rheometer. Granules with a diameter of 5–7 mm were obtained on a laboratory drum granulator.

The granules were molded by rolling in a laboratory granulator (Figure 5). The granules were rolled by loading the raw mixture in two stages. First of all, 85–90% of the entire raw mixture was loaded and mixed with liquid glass. After the formation of the main part of the granule (within 2–3 min) was added 10–15% dry raw mixture. The dry mixture formed a layer on the surface of the wet granules. This prevented the granules from sticking together during rolling.

The productivity of the granulator for this type of raw material was 20 kg in 15 min. The pre-dried granules were fired by placing them in a heated laboratory muffle furnace. Upon completion of firing, the samples were cooled in air. The temperature and duration of heat treatment of the samples were set taking into account the objectives of the experiment.

The mode of heat treatment of the granules is shown in Figure 6.

The state of the fired granules was assessed by the nature of the porous structure and density of the granules. The foaming coefficient was calculated as the ratio of the granule diameters after (D_2 , mm) and before (D_1 , mm) firing.

$$K = \frac{D_2}{D_1}$$

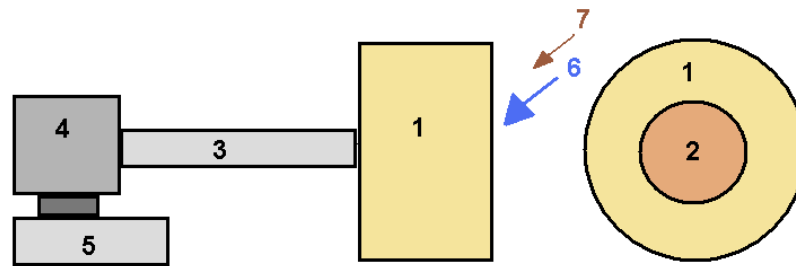


Figure 5. Schematic diagram of the laboratory granulator: 1—drum (diameter 700 mm, width 450 mm); 2—loading opening (diameter 350 mm), 3—shaft; 4—gearbox, 5—electric motor; 6—raw mixture containing liquid glass; 7—dry raw mix.

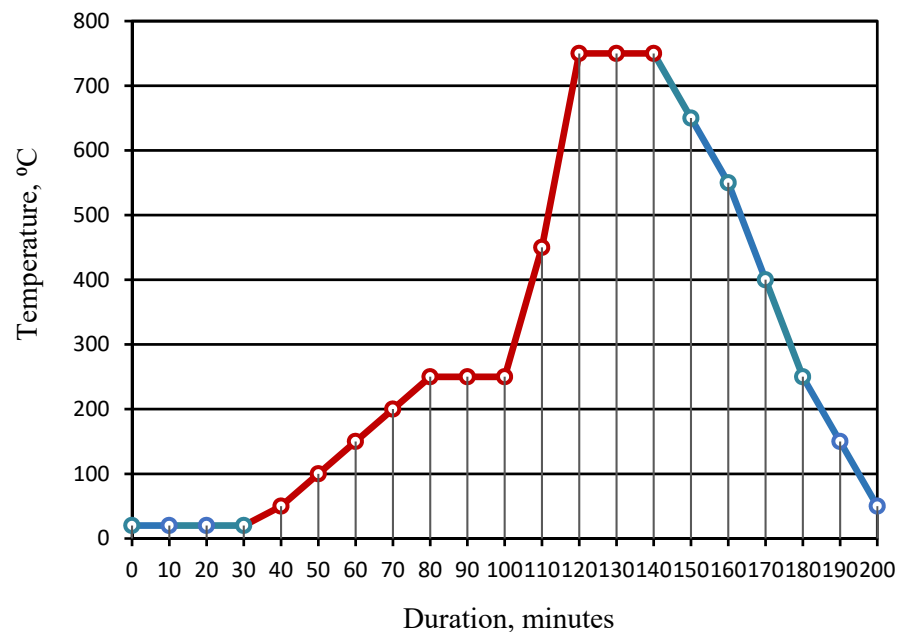


Figure 6. Mode of heat treatment of the granules: 1—pre-drying of raw granules; 2—heating to a temperature of 250 °C; 3—isothermal heating at a temperature of 250 °C (preliminary foaming); 4—heating to a temperature of 750 °C; 5—isothermal heating at a temperature of 750 °C (foaming); 6—cooling.

The average pore size was determined as the average result of nine measurements in the photograph of the granule cleavage.

Pyrogenic transformations in the raw mixture were studied by derivatographic thermal analysis, which was carried out on a modernized device Derivatograph Q-1500 (Paulik-Erdey, Hungary). To determine the phase composition of the materials under study, an upgraded DRON-3M diffractometer (Burevestnik, Russia) was used. The diffractometer is equipped with a BSV-24 type X-ray tube with CuK α -radiation. Diffraction patterns were processed using difWin software. The microstructure of the materials was studied using a JSM-6490LV energy scanning electron microscope (JEOL, Japan). The properties of granular materials were determined according to generally accepted methods.

The total porosity (P , %) of the granules was determined based on the true density of the granule substance (ρ_t , kg/m³) and the bulk density of the granule (ρ_a , kg/m³):

$$P = \frac{\rho_t - \rho_a}{\rho_t} 100$$

The true density of the granule substance was determined by the pycnometric method. The bulk density of the granule (ρ_a , kg/m³) was determined as the ratio of the mass (m ,

kg) to the volume of the granule, for the calculation of which the diameter of the granule (D , m) was determined:

$$\rho_a = \frac{m}{\frac{\pi \cdot D^3}{6}}$$

The values of density and porosity of the studied granules are given in Table 3. The total pore volume of the granules from the proposed mixtures is comparable to the porosity of the foam glass (composition C).

Table 3. Values of the total porosity of granules from raw mixtures of various compositions.

Mix ID	True Density of the Granule Substance, kg/m ³	Bulk Density of the Granule, kg/m ³	Porosity of the Granule, %
C	2650	340	87.2
CB11	2810	330	88.3
CB21	2650	350	86.8
CB31	2780	335	87.9

3. Results and Discussion

3.1. Thermal Foaming of Materials

The ability of raw materials to foam thermally was investigated. The investigated materials were mixed with liquid glass at a ratio of 60:40 wt %, providing a mixture for molding stable granules.

Drying of raw granules was carried out in air at a temperature of 22–25 °C to strengthen the surface layer of the granules. The holding time of the granules is 30–40 min. Heat treatment of raw granules at a temperature of 100–105 °C is impractical, since it is accompanied by an increase in volume due to partial removal of adsorbed water. Such changes in the state of the granules before firing are not provided for by this experiment. The granules, pre-dried in air at a temperature of 22–25 °C, were fired at temperatures of 450, 650, and 850 °C with isothermal holding for 15 min. The mixture of glass breakage and liquid glass used in traditional technology served as the benchmark. The greatest transformations of the samples were noted after firing at a temperature of 850 °C. The moisture content of the molded granules before drying is 15–20%, and after drying, the moisture content of the dried granules tends to zero. Low values of moisture prevent granules from sticking together.

Comparison of the properties of fired samples showed that granules from glass breakage are distinguished by the greatest foaming (Figure 7). Most of the pores in the pyroplastic glass mass are formed by the gas phase due to the dehydration of liquid glass. The experimental conditions did not provide for a special cooling regime used in the foam glass technology; therefore, the expanded granules from the glass breakage were characterized by fragility.

The foaming and structure of fired lignite clay-based granules are similar to those of the gum ones. Despite the lower values of the foaming coefficient, the number of pores in granules from lignite clay is 15–20% more than in granules from opoka rock. Pores in granules are formed not only with the participation of the gas phase released during the dehydration of liquid glass and aluminum hydroxides, but also due to the burnout of carbonized wood.

The thermal transformation of the mixture based on the wastes of enrichment of skarn-magnetite ores is very specific. Specimens fired in the investigated temperature range are characterized by shrinkage. The ratio of the granule sizes before and after firing is 0.81–0.95, taking into account the temperature (Figure 8). At a temperature of 850 °C, sintered structure is formed, the porous structure of which is formed due to gaseous products of dehydration of aluminosilicates, decomposition of pyrite, and calcite. An insignificant number of predominantly large cavities represent the pores. With an increase in the proportion of liquid glass to 55–65% during firing, a melted mass with

pores of various shapes and sizes is formed. The peculiarities of the formation of the structure of granules from ore dressing wastes are due to the low-temperature formation of a mobile melt.

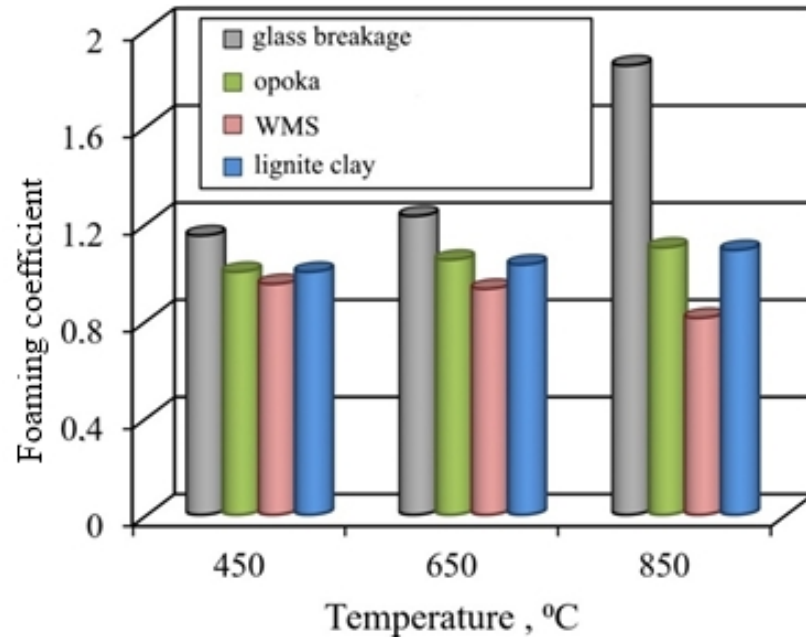


Figure 7. Influence of temperature on the foaming of granules from liquid glass mixtures with various fillers.

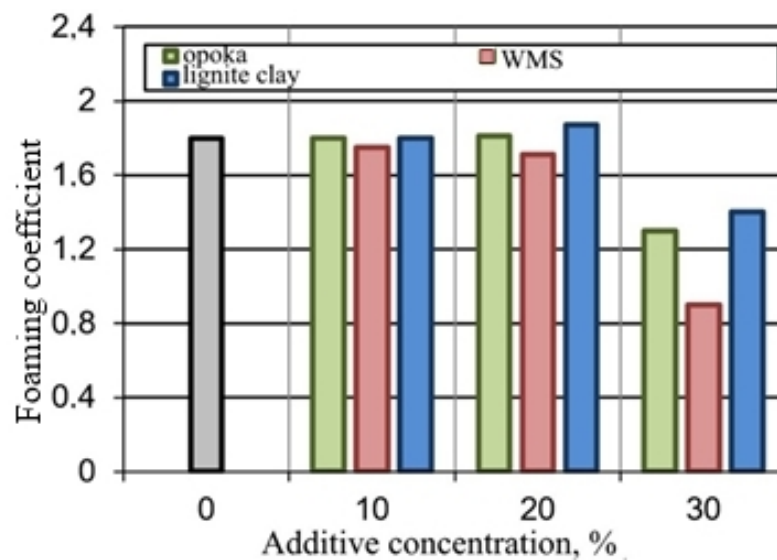


Figure 8. Influence of additives on the foaming of the glass mass.

The experimental results confirmed the possibility of the formation of the porous structure of the mixtures under study due to the liquid glass blowing agent and substances exhibiting thermal activity with the release of the gas phase. However, mixtures with opoka rock and lignite clay do not form a pyroplastic mass in a given temperature range, which prevents foaming. The mixture containing the wastes from enrichment of skarn-magnetite ores, during firing, turns into a melt, from which the gas phase is easily removed.

To realize the pore-forming ability of the materials under study, they were added to a mixture of breakage glass and liquid glass (Table 2, Figure 8). Mixtures containing up

to 20% of opoka rock and lignite clay, at a temperature of 850 °C, are characterized by a foaming coefficient equal to or higher than that for breakage glass. The porosity of C1 expanded granules is comparable to foam glass C (Figure 9). The black color of the fired sample containing ore dressing wastes (Figure 9c) is due to the increased content of ferrous compounds (Table 1).

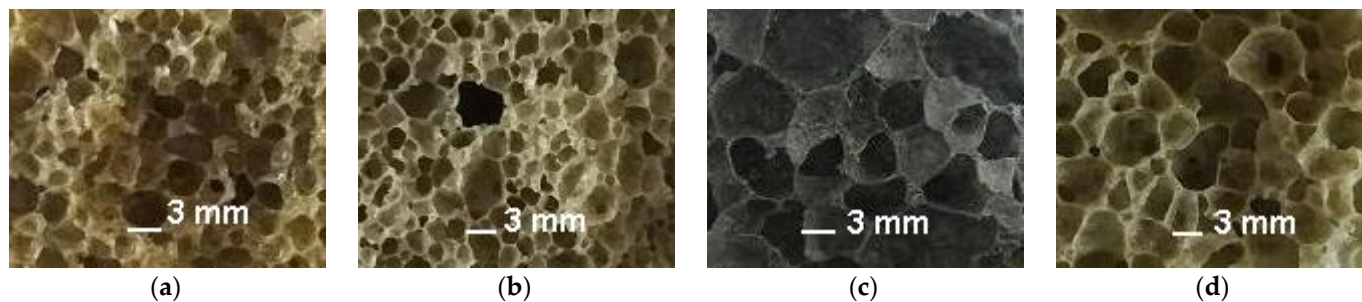


Figure 9. The structure of expanded glass mass granules: (a) without additives; (b) with opoka; (c) with WMS; (d) with lignite clay.

The addition of waste from magnetic separation of skarn-magnetite ores to breakage glass is accompanied by a decrease in the viscosity of the pyroplastic mass, and, as a consequence, the formation of large pores in the C2 granules. The largest values of the foaming coefficient were achieved with the introduction of lignite clay, which is characterized by a high content of gas-forming substances. This caused an increase in the pore size in the structure of the C3 granules.

3.2. Porization of Granules Obtained from Multicomponent Mixes

The introduction of additives has an ambiguous effect on the technological properties of the raw mixture. The addition of gum rock helped to harden the raw granules. Forming granules from glass masses with the addition of lignite clay and especially ore dressing wastes has become difficult. To improve the quality of raw and expanded granules, a combination of additives of various compositions is proposed. The introduction of combined additives reduced the content of breakage glass in the dry mixture to 60% (Table 2). The change in the material composition of the dry mixture made it necessary to increase the liquid glass to 45% of the molding mass. With an increase in the proportion of the liquid component, the molding mass slowly hardened. It is known [49] that sodium salts are used to increase the viscosity of liquid glass compositions. The addition of 3% sodium carbonate (Na_2CO_3) to the molding mixture contributed to the hardening of the raw granules by 27–41% (Table 2), as well as a decrease in the softening temperature of the mass (Table 3). The granules were also fired in the 700–850 °C temperature range, which is characterized by the most intense foaming. A decrease in the density of the fired granules indicates structural changes in the materials (Table 3).

The lowest density values are characteristic of granules with high porosity. For mixtures of CB1 and CB3 containing ore dressing wastes, the lowest density of granules is achieved at temperatures, respectively, 50 and 25 °C lower than for glass mass C. Due to the addition of Na_2CO_3 , the maximum porosity of granules of compositions CB11 and CB31 is achieved at temperatures of 725 and 750 °C. The nature of the thermal changes of granules from a mixture of CB2 has similarities with the reference composition C. With the addition of sodium carbonate, the lowest value of the density of granules of composition CB21 was noted at a temperature of 775 °C. The effect of temperature on the foaming of granules of various compositions (Figure 10) corresponds to temperature changes in the density of the samples (Table 4).

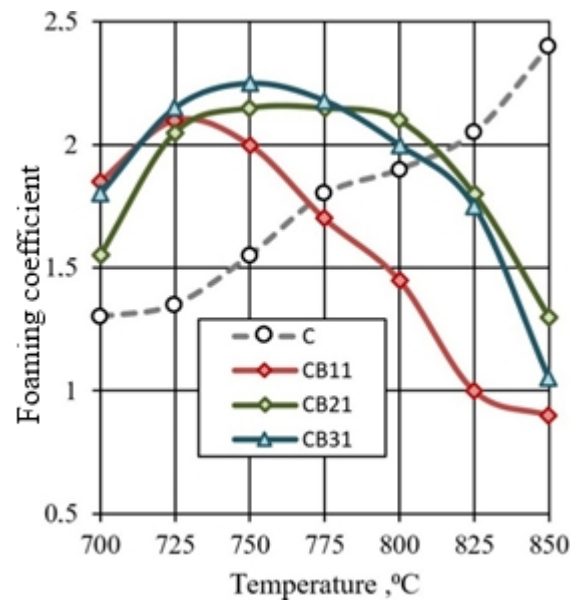


Figure 10. Influence of mixture composition and firing temperature on the granules foaming.

Table 4. Influence of the composition of the mixture and the firing temperature on the density of the granules.

Mix ID	Density of Granules, kg/m ³ , Fired at Temperature, °C						
	700	725	750	775	800	825	850
C	870	765	690	570	440	390	340
CB1	765	585	435	385	335	350	420
CB11	380	330	340	370	440	590	730
CB2	875	740	670	580	455	380	345
CB21	610	455	390	350	360	415	505
CB3	815	655	545	460	390	330	345
CB31	470	385	335	350	390	430	615

Intensive foaming of the CB11, CB21, and CB31 granules containing the addition of sodium carbonate occurs in the 725–775 °C temperature range. The samples have a density of 330–350 kg/m³. An increase in the firing temperature is accompanied by compaction and melting of the granules, and a decrease in the foaming coefficient (Figure 10). This is due to a decrease in the gas-holding capacity of the fired granules: interpore partitions in a mass of low viscosity do not prevent the intense pressure of the gas phase. As a result, shrinkage of the fired samples occurs. This process is pronounced when firing the CB11 mixture, which is characterized by a narrow interval of intense foaming. The high sensitivity of the CB11 mixture to an increase in temperature creates technological problems.

The preference of the CB31 mixture containing a three-component mineral additive is determined by the ability to combine low-temperature foaming with the expansion of the temperature range of the viscous-plastic state of the expanded mass.

The indicators of foaming and density of porous glass-ceramic granules CB11, CB21, and CB31 are comparable to foam glass control mix C. The high porosity of the studied granules from mixtures with a limited proportion of glass is due to the presence of additional sources of gas formation, which is confirmed by the results of thermal analysis (Figure 11). When mixtures are heated in the temperature range of 20–200 °C, 37–47% of the total amount of the gas phase is released. Endothermic effects at temperatures of 90–120 °C indicate the removal of adsorption water from glass breakage, opoka rock, and lignite clay. In the temperature range of 200–500 °C, no significant changes were noted in the DTA pattern of the CB11 mixture (Figure 11a).

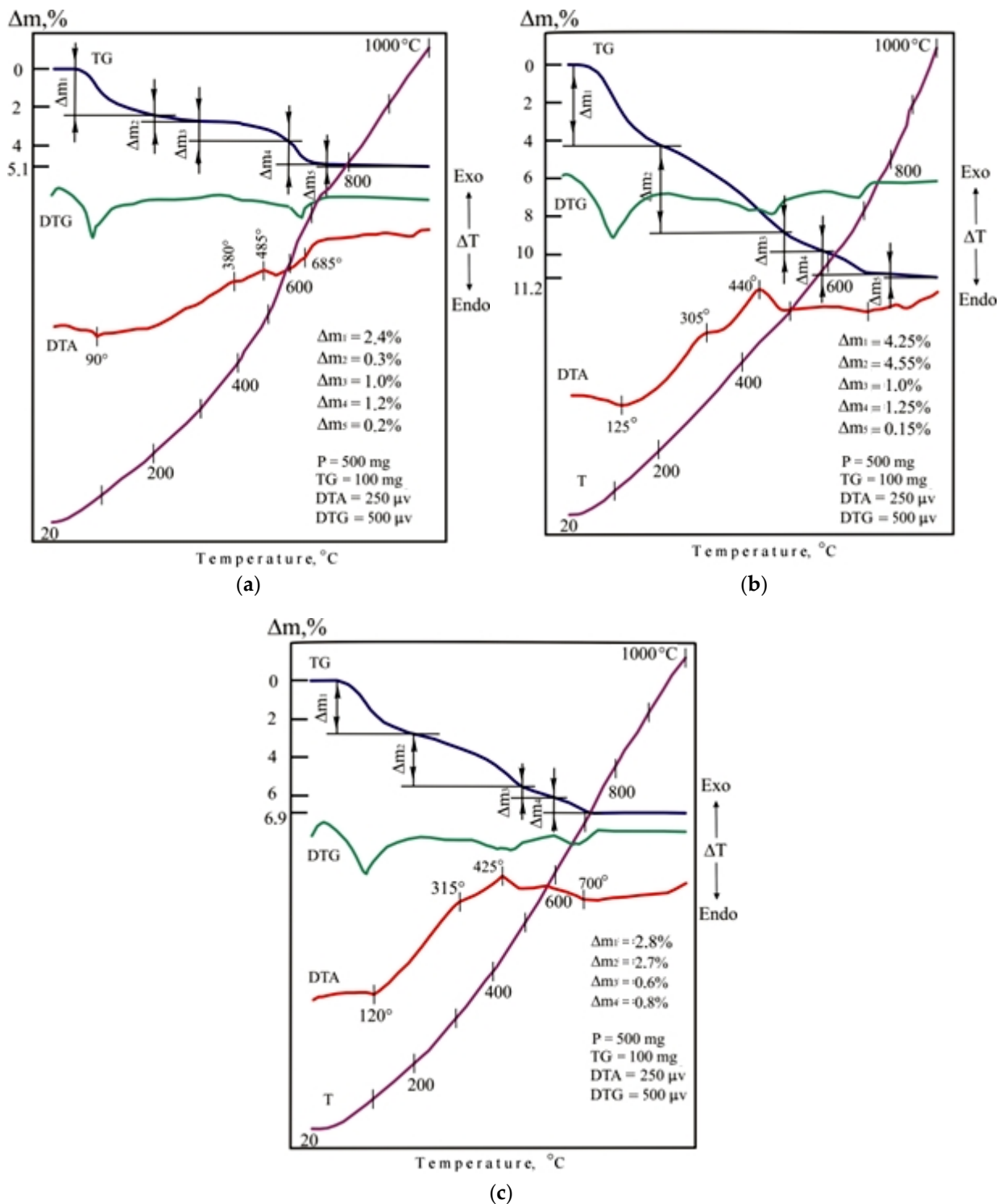


Figure 11. DTA patterns of the dry raw mixtures (without liquid glass): (a) CB11; (b) CB21; (c) CB31.

Taking into account the complex nature of thermal transformations of ore dressing wastes, it can be assumed that the thermal effects accompanying the oxidation of magnetite and pyrite and polymorphic transformations of silica overlap. Heating the CB11 mixture at temperatures from 500 to 800 °C is accompanied by calcite decarbonization, dehydration of actinolite, chlorite, epidote, scapolite, as well as melting of the mixture (endothermic effect at 685 °C).

Heating of mixtures CB21 (Figure 11b) and CB31 (Figure 11c) containing lignite clay in the temperature range of 200–400 °C is accompanied by intense weight loss due to burning out of carbonized wood and partial dehydration of hydrargillite $\text{Al}(\text{OH})_3$ to form boehmite $\text{AlO}(\text{OH})$. When the temperature rises to 600 °C in mixtures of CB21 and CB31, dehydration of boehmite and kaolinite occurs, which is noted in the DTA patterns by endothermic effects at a temperature of 400–500 °C. Firing mixtures CB21 and CB31 in the 600–800 °C temperature range provides gradual softening of the mass. The appearance of a liquid phase in a mixture of C31 containing ore dressing wastes characterizes an extended endothermic effect at a temperature of 700 °C. Melting of the CB21 mixture is completed at a temperature of 810 °C.

The low-temperature formation of the melt in the mixtures under study is due to the content of glass breakage. The amount and viscosity of the liquid phase in the fired mixtures is determined by the mineral composition of the additives. Liquid glass is a component of the studied molding mixtures. When liquid glass is heated, the weight loss is 52–55% due to the removal of free and adsorbed moisture (temperature 115–120 °C), crystallization (temperature 165–170 °C), and hydrated water (temperature 240–245 °C). In the 600–650 °C temperature range, dehydrated sodium silicate decomposes with the formation of silica. Dehydration of liquid glass promotes low-temperature foaming of the mass and the formation of a highly porous structure. When the mixtures under study are heated, liquid glass serves as a source of the main amount of the gas phase.

In addition, in the presence of sodium silicate hydrate, a catalytic acceleration of the dissociation of minerals and the formation of a pyroplastic mass, as well as the emergence of new compounds, is possible. The intensity of such thermal transformations is most likely for mixtures containing polymineral ore dressing wastes. The low-temperature foaming of granules and the phase composition of swollen samples confirm this.

The description of thermal effects in multicomponent mixtures (Figure 11) is hypothetical in nature and is based on thermal analysis data for individual components of the mixture. The transformations in ore dressing wastes were considered by us in the study [23]. The identification of phases in materials fired in the transformation temperature range using X-ray diffraction patterns is difficult due to the polymineral composition of the mixtures. For this study, the results of thermal analysis that characterize processes with a change in the mass of materials are important.

In the XRD pattern of the fired mixture CB31 (Figure 12), reflections of crystalline phases are distinct: mullite (3.363, 2.542, 2.108 Å), cristobalite ($d = 4.105, 3.100, 2.862, 2.481$ Å), calcium-magnesium silicates (3.261, 2.983, 2.542, 2.108 Å), sodium-calcium silicates (4.301, 3.548, 3.100, 2.983, 2.284, 2.108 Å), and anorthite (3.261, 3.100, 2.983, 2.542 Å). In the low-melting multicomponent mixture CB31, containing 3% sodium carbonate, a decrease in the temperature of formation of chemical compounds was noted. This promoted the crystallization of the low-temperature β -modification of cristobalite in the samples under study. The presence of crystalline compounds determines the increased strength of glass-ceramic granules in comparison with foam glass (Table 5).

The rather low thermal conductivity is explained by the closed pore structure of the obtained granules. These results are supported by early studies by various authors [54–57].

The structure of glass crystalline foam granules is characterized by polymodal porosity (Figure 13d–f). Large pores in the center of the granules are predetermined by low-temperature transformations. Drying raw granules at a temperature of 250 °C facilitates their hardening and a 15–20% decrease in the density of granules expanded during firing. Drying is accompanied by primary porosity of granules due to dehydration of liquid glass and removal of adsorbed water from the components of the raw mixture (Figure 13a). During the subsequent firing, the nature of the formation of the porosity of the granules is preserved (Figure 13b,d–f).

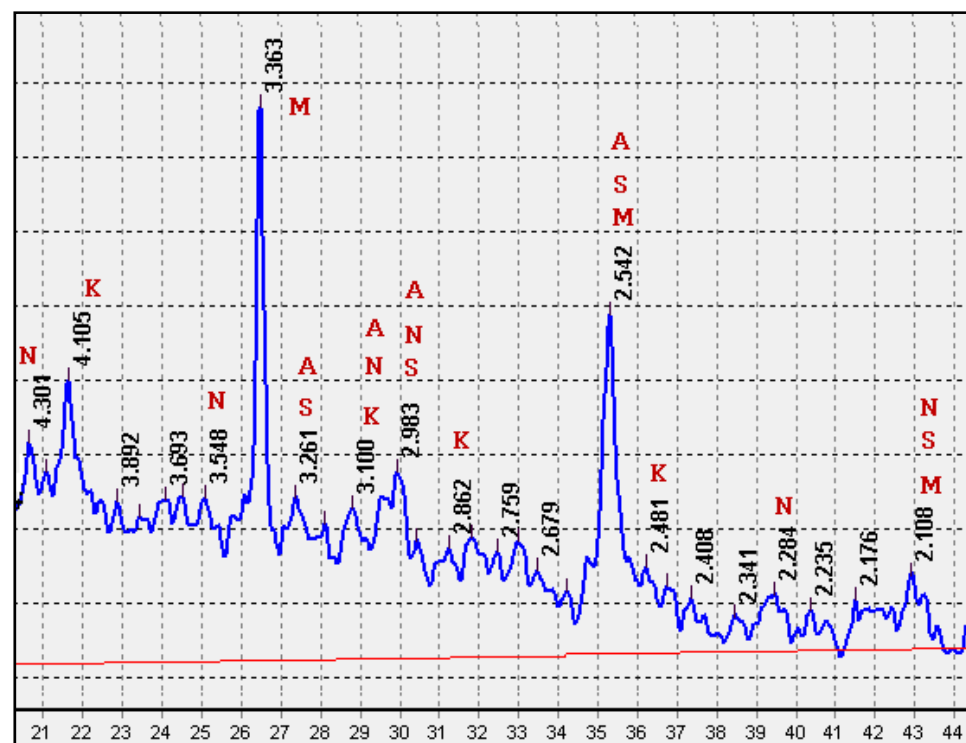


Figure 12. XRD pattern of the CB31 mixture fired at a temperature of 750 °C: M—mullite; K—cristobalite; S—calcium-magnesium silicates; N—sodium-calcium silicates; A—anorthite.

Table 5. Influence of the composition of the molding mixture on the properties of porous granular materials.

Mix ID	Granule Diameter, mm	Granule Density, kg/m ³	Bulk Density of Granules, kg/m ³	Granule Strength, MPa	Water Absorption, %	Coefficient of Thermal Conductivity, W/(m·°C)
C	10–15	340	220	2.1	4.5	0.062
CB11	10–15	330	215	3.4	3.8	0.058
CB21	10–15	350	240	3.2	4.1	0.061
CB31	10–15	335	210	3.7	3.7	0.057

Predominantly closed porosity and smooth surface of expanded granules (Figure 13c) predetermine low water absorption (Table 4).

Large pores, 1–5 mm in size, prevail in the center of the granules. Small cells with a diameter of 0.1–0.2 mm are concentrated along the periphery of the granules. The thickness of the inter-pore partitions does not exceed 10 µm (Figure 14). The smallest cavities with a size of 1–5 µm are located in the walls of large pores. The nature of the porosity of the studied granules is due to the multicomponent composition of the molding mixture, participation in the formation of pores of the gas phase of various origins.

The superficial, less porous layer of the granule serves as a protective sheath for the hollow core. This structure of granules contributes to an increase in the heat-shielding properties of the material (see Table 4). Thus, the developed porous granular material is intended for use as an aggregate for lightweight concretes of low density.

In contrast to the known studies of foam glass obtained from a mixture of glass powder with liquid glass [25,63–67], this work proposes a polymineral mixture for granular material. The expediency of combining glass breakage with wastes of enrichment of skarn-magnetite ores, opoka, and lignite clay was proven by improving the technological properties of the raw mixture, lowering the foaming temperature, and the formation of polymodal porosity of granules. The high porosity of the material from the multicomponent mixture is ensured

with the joint participation of liquid glass and minerals, which form a gas phase during thermal transformations. The presence in the raw mixture of substances with different gas formation temperatures expands the temperature range of granule foaming.

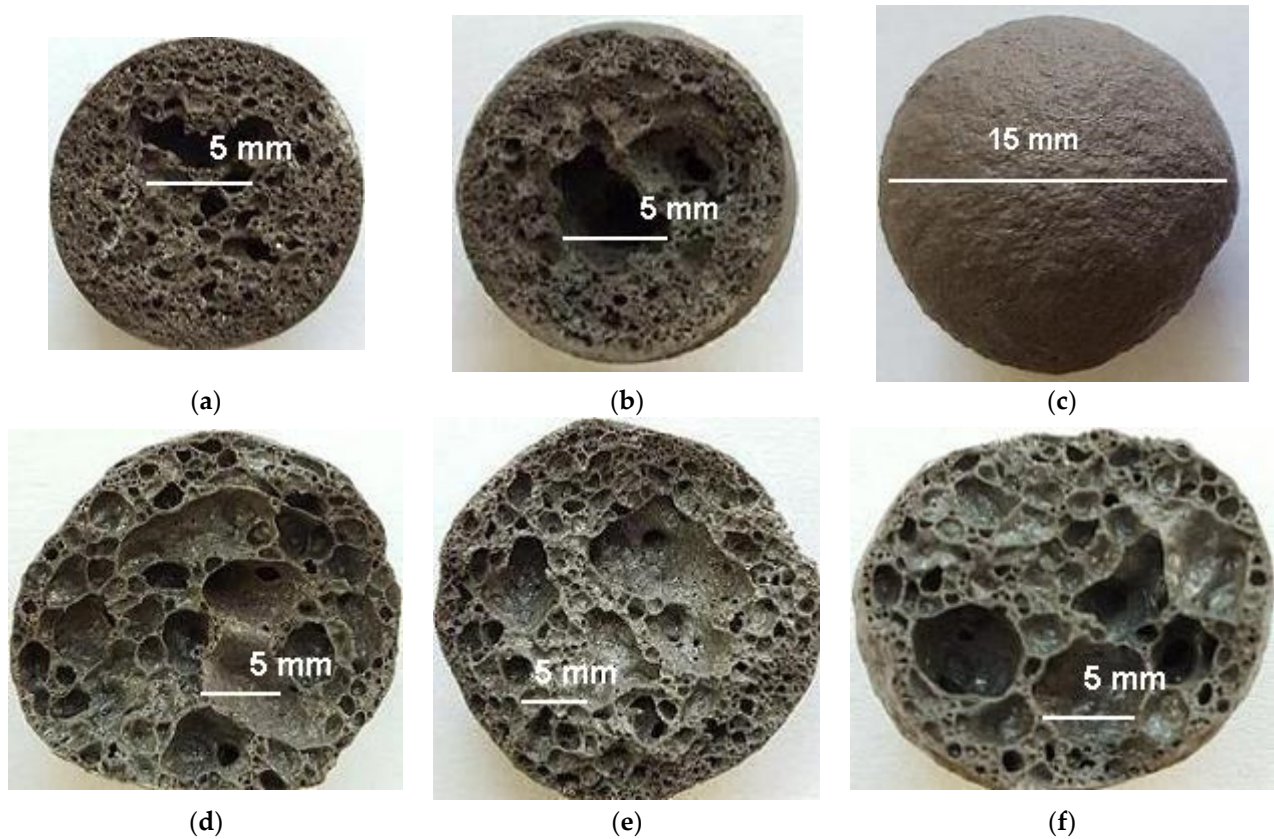


Figure 13. The structure of the fired granules: (a) at a temperature of 250 °C; (b) at a temperature of 550 °C; (c) at a temperature of 750 °C (granule surface); (d) composition of CB11, firing temperature 725 °C; (e) composition of CB21, firing temperature 775 °C; (f) composition of CB31, firing temperature 750 °C.

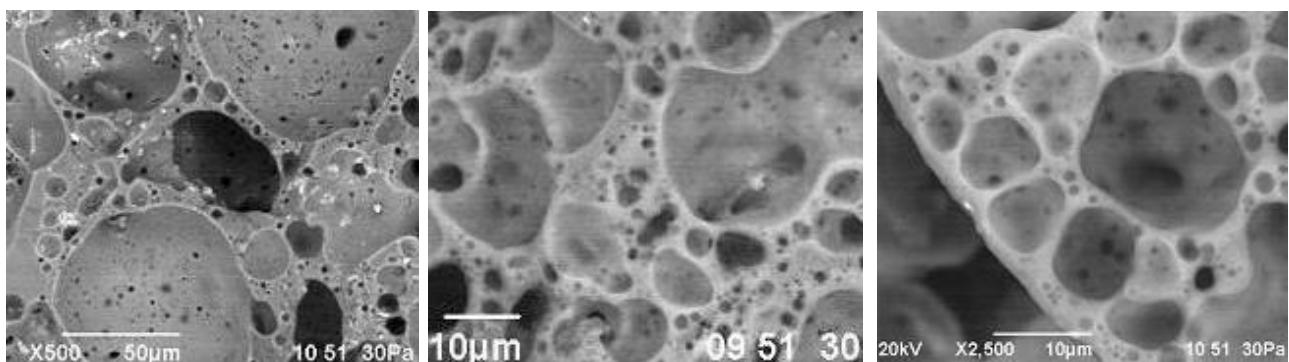


Figure 14. Microstructure of glass-ceramic foam granules from raw mixture CB31.

4. Conclusions

For the first time, scientific results were obtained on the synthesis and properties of glass-ceramic foam granules from a polymineral mixture using magnetic separation waste from skarn-magnetite ores and lignite clay. Analysis of the research results led to the following conclusions.

- Theoretically substantiated and experimentally confirmed the efficiency of using skarn-magnetite ore dressing wastes in the composition of the raw mixture to obtain porous glass-crystalline material. The chemical and mineral composition of the technogenic component provides a decrease in the temperature of the pyroplastic state of the glass mass, the formation of a gas phase due to thermal transformations of minerals and intermediate compounds. The addition of lignite clay containing carbonized wood and aluminum hydroxides to the glass mass promotes an increase in porosity and the formation of crystalline phases in fired granules.
- The expediency of a polymineral molding mixture for obtaining highly porous granules has been proved. The combination of raw materials containing gas-forming substances favors the intensive porosity of the pyroplastic mass. Glass mass with the addition of gum rock, ore dressing waste, and lignite clay allows you to directly influence the molding properties of the raw material mixture, the temperature of granule foaming, and the nature of porosity. The addition of sodium carbonate helps to strengthen the molded granules and lower the softening temperature of the raw material.
- The developed polymineral mixture ensures the formation of stable raw granules with a plastic strength of 0.075 MPa; lowering the foaming temperature of the raw material mass to 750 °C; formation of foam glass-crystalline granules with a density of 330–350 kg/m³, the strength of which is 76% higher than that of foam glass.
- The multicomponent composition of the raw mixture caused the formation of poly-modal porosity of the granules due to the participation of the gas phase of various origins. The central part of the granules, containing closed cavities up to 5 mm in size, is surrounded by a denser shell, in which cells with a diameter of 0.1–0.2 mm are located. In the inter-pore partitions of granules, the smallest cavities with a size of 1–5 μm are concentrated. The structural features of the granules provide high heat-shielding properties of the material, comparable to those of foam glass.
- Prospects for the development of the technology of glass-ceramic granular materials are associated with the further expansion of the raw material base based on a comprehensive study of the composition and properties of materials. It is necessary to improve the methods of molding raw granules, to clarify the mode of heat treatment, and to study the stability of glass-crystalline foam granules in composite materials of various compositions.

Author Contributions: Data curation, M.A., O.M., and R.F.; formal analysis, M.A., O.M., and R.F.; funding acquisition, M.A., O.M., and R.F.; investigation, M.A., O.M., and R.F.; methodology, M.A., O.M., and R.F.; project administration, M.A., O.M., and R.F.; resources, M.A., O.M., and R.F.; software, M.A., O.M., and R.F.; supervision, M.A., O.M., and R.F.; validation, M.A., O.M., and R.F.; visualization, M.A., O.M., and R.F.; writing—original draft, M.A., O.M., and R.F. All authors have read and agreed to the published version of the manuscript.

Funding: This research is funded by the Science Committee of the Ministry of Education and Science of the Republic of Kazakhstan (grant No. AP08856219).

Conflicts of Interest: The authors declare no conflict of interest.

References

1. Wang, X.; Zhang, X.; Song, L.; Zhou, H.; Wang, Y.; Zhang, H.; Cong, P. Mitigating confined blast response of buried steel box structure with foam concrete. *Thin-Walled Struct.* **2021**, *169*, 108473. [[CrossRef](#)]
2. Liu, S.; Zhu, K.; Cui, S.; Shen, X.; Tan, G. A novel building material with low thermal conductivity: Rapid synthesis of foam concrete reinforced silica aerogel and energy performance simulation. *Energy Build.* **2018**, *177*, 385–393. [[CrossRef](#)]
3. Hou, L.; Li, J.; Lu, Z.; Niu, Y.; Jiang, J.; Li, T. Effect of nanoparticles on foaming agent and the foamed concrete. *Constr. Build. Mater.* **2019**, *227*, 116698. [[CrossRef](#)]
4. Huynh, T.-P.; Ho, N.-T.; Bui, P.-T.; Do, N.-D.; Nguyen, T.-C. Mechanical-thermal characteristics of foamed ultra-lightweight composites. *Mag. Civ. Eng.* **2020**, *98*, 9802.
5. Chen, G.; Li, F.; Geng, J.; Jing, P.; Si, Z. Identification, generation of autoclaved aerated concrete pore structure and simulation of its influence on thermal conductivity. *Constr. Build. Mater.* **2021**, *294*, 123572. [[CrossRef](#)]

6. Murali, G.; Abid, S.R.; Karthikeyan, K.; Haridharan, M.; Amran, M.; Siva, A. Low-velocity impact response of novel prepacked expanded clay aggregate fibrous concrete produced with carbon nano tube, glass fiber mesh and steel fiber. *Constr. Build. Mater.* **2021**, *284*, 122749. [[CrossRef](#)]
7. Peng, C.; Kim, Y.J.; Zhang, J. Thermal and energy characteristics of composite structural insulated panels consisting of glass fiber reinforced polymer and cementitious materials. *J. Build. Eng.* **2021**, *43*, 102483. [[CrossRef](#)]
8. Zagorodnyuk, L.; Lesovik, V.S.; Sumskey, D. Thermal insulation solutions of the reduced density. *Constr. Mater. Prod.* **2020**. [[CrossRef](#)]
9. Qu, Y.-N.; Su, Z.-G.; Xu, J.; Huo, W.-L.; Song, K.-C.; Wang, Y.-L.; Yang, J.-L. Preparation of ultralight glass foams via vacuum-assisted foaming. *Mater. Lett.* **2016**, *166*, 35–38. [[CrossRef](#)]
10. Cimavilla-Román, P.; Villafañe-Calvo, J.; López-Gil, A.; König, J.; Rodríguez-Perez, M.A. Modelling of the mechanisms of heat transfer in recycled glass foams. *Constr. Build. Mater.* **2021**, *274*, 122000. [[CrossRef](#)]
11. Bento, A.C.; Kubaski, E.T.; Sequinel, T.; Pianaro, S.A.; Varela, J.A.; Tebcherani, S.M. Glass foam of macroporosity using glass waste and sodium hydroxide as the foaming agent. *Ceram. Int.* **2013**, *39*, 2423–2430. [[CrossRef](#)]
12. König, J.; Petersen, R.R.; Yue, Y. Influence of the glass particle size on the foaming process and physical characteristics of foam glasses. *J. Non-Cryst. Solids* **2016**, *447*, 190–197. [[CrossRef](#)]
13. Hribar, U.; Spreitzer, M.; König, J. Applicability of water glass for the transfer of the glass-foaming process from controlled to air atmosphere. *J. Clean. Prod.* **2021**, *282*, 125428. [[CrossRef](#)]
14. Silva, R.C.; Kubaski, E.T.; Tenório-Neto, E.T.; Lima-Tenório, M.K.; Tebcherani, S.M. Foam glass using sodium hydroxide as foaming agent: Study on the reaction mechanism in soda-lime glass matrix. *J. Non-Cryst. Solids* **2019**, *511*, 177–182. [[CrossRef](#)]
15. Smiljanić, S.; Hrabar, U.; Spreitzer, M.; König, J. Influence of additives on the crystallization and thermal conductivity of container glass cullet for foamed glass preparation. *Ceram. Int.* **2021**, *47*, 32867–32873. [[CrossRef](#)]
16. Østergaard, M.B.; König, R.R.P.J.; Johr, H.; Yu, Y. Influence of foaming agents on solid thermal conductivity of foam glasses prepared from CRT panel glass. *J. Non-Cryst. Solids* **2017**, *465*, 59–64. [[CrossRef](#)]
17. Erofeev, V.T.; Rodin, A.I.; Bochkin, V.S.; Ermakov, A.A. Properties of porous glass ceramics based on siliceous rocks. *Mag. Civ. Eng.* **2021**, *102*, 10202.
18. Monich, P.R.; Romero, A.R.; Hollen, D.; Bernardo, E. Porous glass-ceramics from alkali activation and sinter-crystallization of mixtures of waste glass and residues from plasma processing of municipal solid waste. *J. Clean. Prod.* **2018**, *188*, 871–878. [[CrossRef](#)]
19. Yio, M.; Xiao, Y.; Ji, R.; Russell, M.; Cheeseman, C. Production of foamed glass-ceramics using furnace bottom ash and glass. *Ceram. Int.* **2021**, *47*, 8697–8706. [[CrossRef](#)]
20. Guo, Y.; Zhang, Y.; Huang, H.; Meng, K.; Hu, K.; Hu, P.; Wang, X.; Zhang, Z.; Meng, X. Novel glass ceramic foams materials based on red mud. *Ceram. Int.* **2014**, *40*, 6677–6683. [[CrossRef](#)]
21. Owoeye, S.S.; Matthew, G.O.; Oviemhanda, F.O.; Tunmilayo, S.O. Preparation and characterization of foam glass from waste container glasses and water glass for application in thermal insulations. *Ceram. Int.* **2020**, *46B*, 11770–11775. [[CrossRef](#)]
22. Kurtulus, C.; Kurtulus, R.; Kavas, T. Foam glass derived from ferrochrome slag and waste container glass: Synthesis and extensive characterizations. *Ceram. Int.* **2021**, *47*, 24997–25008. [[CrossRef](#)]
23. Miryuk, O. Thermal transformations in polyminerall technogenic cement raw. *IOP Conf. Ser. Mater. Sci. Eng.* **2020**, *889*, 012025. [[CrossRef](#)]
24. König, J.; Petersen, R.R.; Iversen, N.; Yue, Y. Application of foaming agent–oxidizing agent couples to foamed-glass formation. *J. Non-Cryst. Solids* **2020**, *553*, 120469. [[CrossRef](#)]
25. Hesky, D.; Aneziris, C.G.; Gro, U.; Horn, A. Water and waterglass mixtures for foam glass production. *Ceram. Int.* **2015**, *41*, 12604–12613. [[CrossRef](#)]
26. Goltsman, B.; Yatsenko, L.A.; Goltsman, N.S. Study of the Water-Glass Role in the Foam Glass Synthesis Using Glycerol Foaming Agent. *Diffus. Defect Data Part B Solid State Phenom.* **2021**, *316*, 153–158. [[CrossRef](#)]
27. Bernardo, E.; Elsayed, H.; Rincón Romero, A.; Crovace, M.C.; Zanotto, E.D.; Fey, T. Biosilicate@Glass-Ceramic Foams from Refined Alkali Activation and Gel Casting. *Front. Mater.* **2021**, *7*. [[CrossRef](#)]
28. Siddika, A.; Hajimohammadi, A.; Sahajwalla, V. Powder sintering and gel casting methods in making glass foam using waste glass: A review on parameters, performance, and challenges. *Ceram. Int.* **2021**. [[CrossRef](#)]
29. Vaysman, Y.I.; Ketov, A.A.; Ketov, P.A. Secondary Application of Foam Glass when Producing Foam-Glass-Crystal Slabs. *Stroit. Mater.* **2017**, *748*, 56–59. [[CrossRef](#)]
30. Akai, T.; Fukumi, K.; Yamashita, M. Formation of pale foam glass from colored glass cullet. *J. Ceram. Soc. Jpn.* **2020**, *128*, 153–157. [[CrossRef](#)]
31. Liu, Y.; Xie, J.; Hao, P.; Shi, Y.; Xu, Y.; Ding, X. Study on Factors Affecting Properties of Foam Glass Made from Waste Glass. *J. Renew. Mater.* **2021**, *9*, 237–253. [[CrossRef](#)]
32. Kim, E.; Kim, K.; Song, O. Properties of foamed glass upon addition of polysiloxane. *J. Asian Ceram. Soc.* **2020**, *8*, 930–938. [[CrossRef](#)]
33. Kazmina, O.; Semukhin, B.; Elistratova, A. Strengthening of Foam Glass Materials. *Adv. Mater. Res.* **2013**, *872*, 79–83. [[CrossRef](#)]
34. Azreen, N.M.; Raizal, S.M.R.; Haniza, M.; Voo, Y.L.; Amran, Y.H.M. Radiation shielding of ultra-high-performance concrete with silica sand, amang and lead glass. *Constr. Build. Mater.* **2018**, *172*, 370–377. [[CrossRef](#)]

35. Loutou, M.; Hajjaji, M.; Mansori, M.; Favotto, C.; Hakkou, R. Phosphate sludge: Thermal transformation and use as lightweight aggregate material. *J. Environ. Manag.* **2013**, *130*, 354–360. [[CrossRef](#)] [[PubMed](#)]
36. Adhikary, S.K.; Rudžionis, Ž.; Tučkutė, S.; Ashish, D.K. Effects of carbon nanotubes on expanded glass and silica aerogel based lightweight concrete. *Sci. Rep.* **2021**, *11*, 2104. [[CrossRef](#)] [[PubMed](#)]
37. Roces, E.; Muñiz-Menéndez, M.; González-Galindo, J.; Estaire, J. Lightweight expanded clay aggregate properties based on laboratory testing. *Constr. Build. Mater.* **2021**, *313*, 125486. [[CrossRef](#)]
38. Ogawa, Y.; Bui, P.T.; Kawai, K.; Sato, R. Effects of porous ceramic roof tile waste aggregate on strength development and carbonation resistance of steam-cured fly ash concrete. *Constr. Build. Mater.* **2020**, *236*. [[CrossRef](#)]
39. Liu, T.; Tang, Y.; Han, L.; Song, J.; Luo, Z.; Lu, A. Recycling of harmful waste lead-zinc mine tailings and fly ash for preparation of inorganic porous ceramics. *Ceram. Int.* **2017**, *43*, 4910–4918. [[CrossRef](#)]
40. Fedyuk, R.S.; Baranov, A.V.M.; Amran, Y. Effect of porous structure on sound absorption of cellular concrete. *Constr. Mater. Prod.* **2020**, *3*, 5–18.
41. Amran, M.; Lee, Y.H.; Vatin, N.; Fediuk, R.; Poi-Ngian, S.; Lee, Y.Y.; Murali, G. Design efficiency, characteristics, and utilization of reinforced foamed concrete: A review. *Crystals* **2020**, *10*, 948. [[CrossRef](#)]
42. Lesovik, V.; Voronov, V.; Glagolev, E.; Fediuk, R.; Alaskhanov, A.; Amran, Y.M.; Murali, G.; Baranov, A. Improving the behaviors of foam concrete through the use of composite binder. *J. Build. Eng.* **2020**, *31*, 101414. [[CrossRef](#)]
43. Amran, Y.M.; Alyousef, R.; Alabduljabbar, H.; Khudhair, M.H.R.; Hejazi, F.; Alaskar, A.; Alrshoudi, F.; Siddika, A. Performance properties of structural fibred-foamed concrete. *Results Eng.* **2020**, *5*, 100092. [[CrossRef](#)]
44. Amran, Y.M. Influence of structural parameters on the properties of fibred-foamed concrete. *Innov. Infrastruct. Solut.* **2020**, *5*, 1–18. [[CrossRef](#)]
45. Fediuk, R.; Amran, M.; Vatin, N.; Vasilev, Y.; Lesovik, V.; Ozbakkaloglu, T. Acoustic Properties of Innovative Concretes: A Review. *Materials* **2021**, *14*, 398. [[CrossRef](#)] [[PubMed](#)]
46. Cerny, V.; Kocianova, M.; Drochytka, R. Possibilities of lightweight high strength concrete production from sintered fly ash aggregate. *Procedia Eng.* **2017**, *195*, 9–16. [[CrossRef](#)]
47. Narattha, C.; Chaipanich, A. Phase characterizations, physical properties and strength of environment-friendly cold-bonded fly ash lightweight aggregates. *J. Clean. Prod.* **2018**, *171*, 1094–1100. [[CrossRef](#)]
48. Gomathi, P.; Sivakumar, A. Accelerated curing effects on the mechanical performance of cold bonded and sintered fly ash aggregate concrete. *Constr. Build. Mater.* **2015**, *77*, 276–287. [[CrossRef](#)]
49. Borowski, G.; Ozga, M. Comparison of the processing conditions and the properties of granules made from fly ash of lignite and coal. *Waste Manag.* **2020**, *104*, 192–197. [[CrossRef](#)]
50. Niu, Y.-H.; Fan, X.-Y.; Ren, D.; Wang, W.; Li, Y.; Yang, Z.; Cui, L. Effect of Na₂CO₃ content on thermal properties of foam-glass ceramics prepared from smelting slag. *Mater. Chem. Phys.* **2020**, *256*, 123610. [[CrossRef](#)]
51. Onaizi, A.M.; Lim, N.H.A.S.; Huseien, G.F.; Amran, M.; Ma, C.K. Effect of the addition of nano glass powder on the compressive strength of high volume fly ash modified concrete. *Mater. Today Proc.* **2021**. [[CrossRef](#)]
52. Kasemchaisiri, R.; Tangtermsirikul, S. A method to determine water retainability of porous fine aggregate for design and quality control of fresh concrete. *Constr. Build. Mater.* **2007**, *21*, 1322–1334. [[CrossRef](#)]
53. Rashad, A.M. Recycled waste glass as fine aggregate replacement in cementitious materials based on Portland cement. *Constr. Build. Mater.* **2014**, *72*, 340–357. [[CrossRef](#)]
54. Kazmina, O.V.; Mitina, N.A.; Minaev, K.M. Lightweight cement mortar with inorganic perlite microspheres for equipping oil and gas production wells. *Mag. Civ. Eng.* **2020**, *93*, 83–96.
55. Yildirim, H.; Özturan, T. Impact resistance of concrete produced with plain and reinforced cold-bonded fly ash aggregates. *J. Build. Eng.* **2021**, *42*, 102875. [[CrossRef](#)]
56. Li, X.; He, C.; Lv, Y.; Jian, S.; Liu, G.; Jiang, W.; Jiang, D. Utilization of municipal sewage sludge and waste glass powder in production of lightweight aggregates. *Constr. Build. Mater.* **2020**, *256*, 119413. [[CrossRef](#)]
57. Moghadam, M.J.; Ajalloeian, R.; Hajiannia, A. Preparation and application of alkali-activated materials based on waste glass and coal gangue. *Constr. Build. Mater.* **2019**, *221*, 84–98. [[CrossRef](#)]
58. Rodríguez-Álvaro, R.; Seara-Paz, S.; González-Fonteboa, B.; Etxeberria, M. Study of different granular by-products as internal curing water reservoirs in concrete. *J. Build. Eng.* **2021**, *45*, 103623. [[CrossRef](#)]
59. Song, H.; Chai, C.; Zhao, Z.; Wei, L.; Wu, H.; Cheng, F. Experimental study on foam glass prepared by hydrothermal hot pressing-calcination technique using waste glass and fly ash. *Ceram. Int.* **2021**, *47*, 28603–28613. [[CrossRef](#)]
60. Usanova, K.; Barabanshchikov, Y.G. Cold-bonded fly ash aggregate concrete. *Mag. Civ. Eng.* **2020**, *95*, 104–118. [[CrossRef](#)]
61. Korsun, V.; Vatin, N.; Korsun, A.; Nemova, D. Physical-mechanical properties of the modified fine-grained concrete subjected to thermal effects up to 200 °C. *Appl. Mech. Mater.* **2014**, *633–634*, 1013–1017. [[CrossRef](#)]
62. Elistratkin, M.Y.; Lesovik, V.S.; Zagorodnjuk, L.H.; Pospelova, E.A.; Shatalova, S.V. New point of view on materials development. *IOP Conf. Ser. Mater. Sci. Eng.* **2018**, *327*, 032020. [[CrossRef](#)]
63. Murali, G.; Abid, S.R.; Amran, M.; Fediuk, R.; Vatin, N.; Karelina, M. Combined Effect of Multi-Walled Carbon Nanotubes, Steel Fibre and Glass Fibre Mesh on Novel Two-Stage Expanded Clay Aggregate Concrete against Impact Loading. *Crystals* **2021**, *11*, 720. [[CrossRef](#)]

-
64. Murali, G.; Fediuk, R. A Taguchi approach for study on impact response of ultra-high-performance polypropylene fibrous cementitious composite. *J. Build. Eng.* **2020**, *30*, 101301. [[CrossRef](#)]
 65. Chernysheva, N.; Lesovik, V.; Fediuk, R.; Vatin, N. Improvement of Performances of the Gypsum-Cement Fiber Reinforced Composite (GCFRC). *Materials* **2020**, *13*, 3847. [[CrossRef](#)]
 66. Lesovik, V.; Volodchenko, A.; Fediuk, R.; Amran, Y.H.M. Improving the Hardened Properties of Nonautoclaved Silicate Materials Using Nanodispersed Mine Waste. *J. Mater. Civ. Eng.* **2021**, *33*, 04021214. [[CrossRef](#)]
 67. Lesovik, V.; Chernysheva, N.; Fediuk, R.; Amran, M.; Murali, G.; de Azevedo, A.R. Optimization of fresh properties and durability of the green gypsum-cement paste. *Constr. Build. Mater.* **2021**, *287*, 123035. [[CrossRef](#)]